Transient time-averaged spectra of rapidly-modulated semiconductor lasers

M. Osiński, M.Sc., Ph.D., Mem. Polish Phys. Soc., and M.J. Adams, M.Sc., Ph.D., A.R.C.S., A.F.I.M.A.

Indexing terms: *Semiconductor lasers, Lasers*

Abstract: Using the computed solution of multimode rate equations, and including wavelength-chirping effects via the dependence of the refractive index on carrier concentration, it is possible to calculate time-averaged spectra of rapidly-modulated lasers. The averaging time may be used to simulate the effects of measuring equipment with a specific time response. The results show a characteristic fine structure within the dominant longitudinal mode spectrum, and are in qualitative agreement with experimental measurements reported by other authors.

1 Introduction

The dynamic wavelength shift in lasers modulated with a high bit rate gives rise to a fine structure of the emission spectrum that can be revealed in high-resolution measurements. Apart from spectral line broadening, the most striking characteristic is the 'rabbit-ear' nature of the spectrum (see, for example, Reference 1). Near the centre of the spectrum, each longitudinal mode is split into two lines of similar intensity, whereas the side modes are usually asymmetrical with the short-wavelength lobe stronger at the short-wavelength side of the spectrum and vice versa. This structure resembles CW spectra with higher-order transverse modes (cf. Reference 2) and was misinterpreted as being due to the excitation of transverse (lateral) modes in early reports [3, 4]. Subsequently, the commonly observed broadening of mode linewidth in pulsing lasers [1, 5–14] was attributed to the dynamic wavelength shift [1, 8–15] but, apart from a rather qualitative argument by Hakki [1], no detailed analysis of transient time-averaged spectra has been given until recently [16].

Whereas it is now generally accepted that a free-carrier induced variation of the refractive index leads to the linewidth broadening of individual longitudinal modes in pulsing lasers [1, 8–15], the mode-splitting effects seem to be only rarely attributed to the same cause [1, 17]. For example, in Reference 18 reflections from the laser mount are suggested as a reason for the mode splitting in the spectra of gain-switched lasers.

Because of its fundamental nature, the dynamic line broadening should occur in any type of laser, including single-mode distributed-feedback lasers or lasers coupled to external cavities. Transient spectra similar to those observed for AlGaAs lasers have been reported for rapidly modulated [14, 19] and gain-switched [20–22] InGaAsP lasers.

Also, the 'rabbit-ear' lineshape has been observed in quaternary distributed-Bragg-reflector lasers modulated with 2–3 GHz frequency [23], and the mode-splitting effect has been recorded in spectra of 140 Mbit/s-modulated short-external-cavity lasers [19]. Most recently a similar effect was observed in high-resolution spectra of single-mode 1.5 μm cleaved-coupled-cavity (C^3) lasers modulated at 100 MHz [17].

In the present paper, numerical calculations are presented of transient time-averaged spectra of rapidly-modulated 1.55 μm lasers. These are obtained from computer solutions of multimode rate equations using a newly-developed averaging procedure. An account of the model used to describe the dynamic interaction of photon and electron populations in the laser is given in Section 2; the response to a 0.5 ns current pulse is investigated as a specific case of interest. In Section 3 the details of the time-averaging procedure are given. Some results using this procedure have already been presented in a preliminary report [16]. New results are presented in Section 4 where we confine attention to the time-averaged behaviour of a single longitudinal mode. The computed behaviour is in qualitative agreement with experimental measurements reported by other authors [17, 24].

2 Model for transient behaviour

Transient solutions of multimode rate equations for electron and photon populations have been discussed in our earlier publications [25, 26]. The model used for radiative transitions is that for band-to-band recombination with no k-selection rule, including the effects of bandgap shrinkage [27]. This model is common to the calculation both of gain and of the spontaneous emission coupling coefficient β; this latter quantity is scaled to have a value of 10^{-5} for the dominant mode. The calculations reported here were performed for a 1.55 μm InGaAsP index-guided laser with a cavity length of 200 μm.

Fig. 1 shows the computed transient evolution of the single-ended power output in the dominant mode in response to a trapezoidal current pulse. This modulation current pulse (broken line in Fig. 1) has a halfwidth of 0.5 ns, rise and fall times of 50 ps, a maximum value of 90% of the threshold current, and is superimposed on a bias current of 1.1 times threshold. Under prebias conditions, the ratio of dominant to secondary mode intensities is 12 : 1; both the secondary modes situated on either side of the dominant one have equal power. The ratio of dominant to secondary mode intensities is approximately maintained for the duration of the current pulse. Although this is no longer the case after the end of the pulse, the power in the modes then is so low (note the logarithmic scale on Fig. 1) as not to influence the average spectra.

Paper 3547J (E13, E3), first received 8th August and in revised form 3rd October 1984

Dr. Osiński was formerly with the Department of Electronics, University of Southampton, and is now with the University of Cambridge Engineering Department, Trumpington Street, Cambridge CB2 1PZ, England. Dr. Adams is with BTRL, Martlesham Heath, Ipswich IP5 7RE, England

Thus, whilst 15 modes are included in the calculation, we concentrate here only on results for the dominant mode.

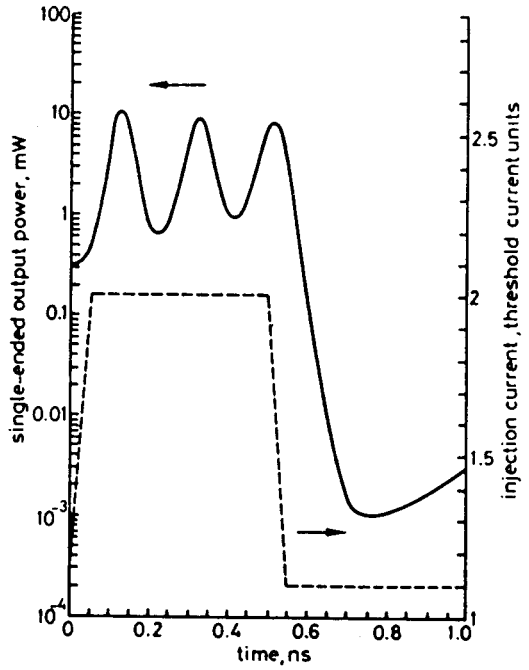

Fig. 1 *Transient evolution of single-ended laser output in the dominant mode of a 1.55 μm InGaAsP laser (200 μm cavity length) calculated from numerical solution of multimode rate equations*

The broken line shows the modulation current pulse

The transient evolution of power shown in Fig. 1 is accompanied by a time-dependent variation of the mode wavelength which must also be considered in calculating the time-averaged spectra. The free-carrier induced refractive index variation ($d\mu/dn$) is a key parameter in determining the magnitude of wavelength-chirping in modulated lasers. The experimental evaluation of $d\mu/dn$ is not easy, since it requires a knowledge of the electron concentration. Measurements on 1.3 μm lasers by Turley [28] suggest that $d\mu/dn$ in this material varies between $-(2-3.3)\times10^{-20}$ cm^3 if $n_{th}=1.7\times10^{18}$ cm^{-3} is assumed at threshold as obtained from our model for gain [27]. This estimate agrees very well with more recent measurements of Manning *et al.* [29] who obtained $d\mu/dn=-(2.8\pm0.6)\times10^{-20}$ cm^3 for 1.3 μm InGaAsP lasers.

New data on the carrier-induced wavelength shift in 1.55 μm planar stripe lasers reported by Bouley *et al.* [30] lead us to a similar estimate of $d\mu/dn$ as mentioned above. The total observed wavelength change from zero bias level to the threshold ranged between 75 and 100 Å. This seems to be compatible with the carrier-induced wavelength shift of 98 Å reported for 1.6 μm BH lasers by Kishino *et al.* [15]. The values given by Bouley *et al.* [30], if corrected for the temperature increase under CW conditions, would become larger than that given by Kishino *et al.* [15], which should be expected since the threshold electron concentration in planar stripe lasers is higher than in buried lasers [31]. However, the fact that Bouley *et al.* [30] have neglected the heat-induced wavelength shift means that their value for $d\mu/dn=-1.5\times10^{-20}$ cm^3 may be an underestimate. On these grounds we decided to use our estimate of $d\mu/dn=-2.8\times10^{-20}$ cm^3 in the calculations recounted here.

The wavelength-chirping occurring simultaneously with the power evolution of Fig. 1 is shown in Fig. 2. It is the combination of output power ringing and wavelength-chirping shown in these Figures which gives rise to the characteristic 'rabbit-eared' spectra showed in rapidly-modulated lasers. In order to simulate such spectra we have originated a technique for calculating the time-averaged power spectral density, the details of which are given in the following section.

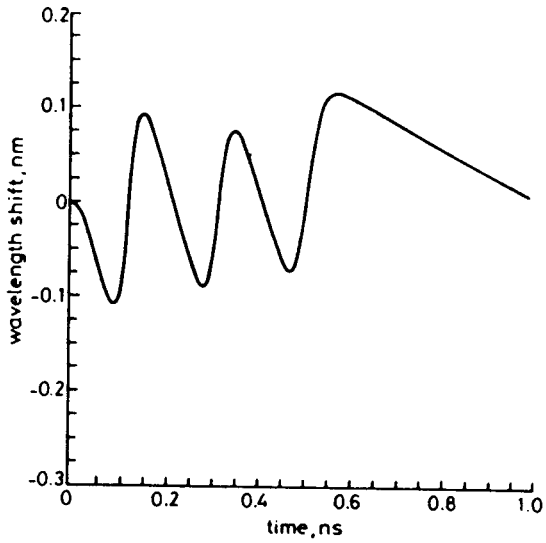

Fig. 2 *Wavelength-chirping calculated for the same case as Fig. 1*

3 Description of numerical method

The time-averaged power spectrum can be obtained from the numerical solution of multimode rate equations using the computed time evolution of the power $P_i(t)$ and the wavelength $\lambda_i(t)$ for a given mode i. In order to characterise transient time-averaged spectra, we introduce the power spectral density function defined as

$$\Pi_i(\lambda_i, \Delta t)=\frac{P_i(t)}{\Delta t}\frac{\delta t}{\delta\lambda_i} \tag{1}$$

where λ_i, t are lying in the middle of small intervals $\delta\lambda_i$, δt and Δt is the averaging time. Thus by integrating $\Pi_i(\lambda_i, \Delta t)$ the power $\bar{P}_i(\Delta t)$ averaged over the time slot Δt is obtained:

$$\bar{P}_i(\Delta t)=\int_{\Delta\lambda_i}\Pi_i(\lambda_i, \Delta t)\,d\lambda_i \tag{2}$$

A sketch in Fig. 3 illustrates the numerical method

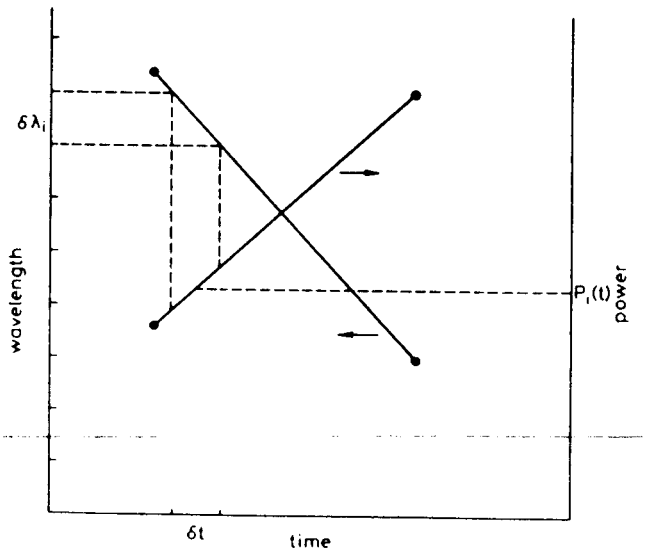

Fig. 3 *Sketch to illustrate the method used for computing the power spectral density as defined in eqn. 1*

adopted for computing $\Pi_i(\lambda_i, \Delta t)$ by linear interpolation of data obtained from the rate equations. Each full dynamic linewidth $\Delta\lambda_i$ over the period Δt is divided into an appropriate number of channels and contributions to each channel are added by analysing the data for $P_i(t)$, $\lambda_i(t)$ step by step. The wavelength axis in Fig. 3 is thus divided into separate channels, and the broken lines demonstrate how the time interval δt, corresponding to the wavelength variation of $\delta\lambda_i$, is determined. The full circles are computed solutions of the rate equations at the beginning and at the end of a sufficiently small time step (1 ps in our case). The energy emitted into each channel during each time step is calculated from the linearly-interpolated time-dependent mode power. Contributions to the channel energy from all time steps are summed together and scaled according to eqn. 1 in order to obtain the power spectral density.

The choice of the channel-width $\delta\lambda_i$ strongly affects values of $\Pi_i(\lambda_i, \Delta t)$ at times when λ_i varies slowly. In order to obtain spectra equivalent to those measured experimentally, the width of a single channel should be equal to the linewidth (FWHM) of the laser operating CW. On the basis of published CW spectra for 1.55 μm lasers [32–34], the value of 0.03 Å (about 380 MHz) was chosen as a channel width, although it should be noted that a linewidth of the order of 100 MHz has also been measured in some samples [32].

It is worth noting that the method developed for calculating the time-averaged spectra does not require excessive computing. In the longest of the cases presented here, it took less than 0.4 s on a CDC 7600 computer to obtain a power spectral density averaged over 700 time steps (each of 1 ps) with the mode linewidth divided into 75 channels.

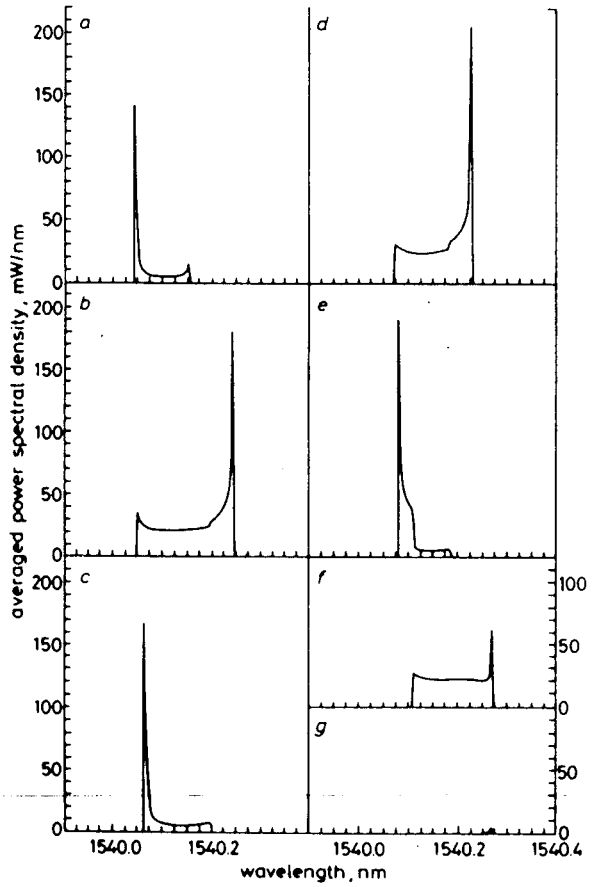

Fig. 4 *Time-resolved spectra calculated by the method described in the text*

Initial and final times for each averaging process were as follows: *a* 0–100 ps, *b* 100–200 ps, *c* 200–300 ps, *d* 300–400 ps, *e* 400–500 ps, *f* 500–600 ps, *g* 600–700 ps. Other parameters as for Figs. 1 and 2.

4 Time-resolved spectra

The power spectral densities obtained from Figs. 1 and 2 by the averaging technique described in the preceding Section are shown in Figs. 4 and 5. Fig. 4 gives time-resolved spectra obtained at different times into the pulse with averaging time of 100 ps in each case. In Fig. 4*a* we see the effect of the first output spike where the power is emitted primarily at shorter wavelengths. The subsequent plots of Figs. 4*b–e* illustrate the ringing oscillations and corresponding power transfer between short and long wavelengths. Fig. 4*f* gives the results on switch-off of the modulation current pulse, while Fig. 4*g* represents residual power on return to pre-bias conditions. We may compare these calculated results with the analogous measured time-resolved spectra reported recently by Linke [24]. Whereas our results show pronounced ringing effects, the relaxation oscillations for Linke's C^3-device are very heavily damped. Thus the measured spectra show strong chirp effects only on start-up (corresponding to Fig. 4*a*) and shut-down (Fig. 4*f*), in agreement with our calculations. The spectral resolution in Linke's measurements [24] was quoted as 0.7 Å and presumably this led to a smoothing out of the 'rabbit ears' so clearly evident in Fig. 4.

Fig. 5 illustrates the evolution of the total averaged power spectrum from the beginning of the pulse. Each graph (*a–g*) extends the averaging time by 100 ps. Thus

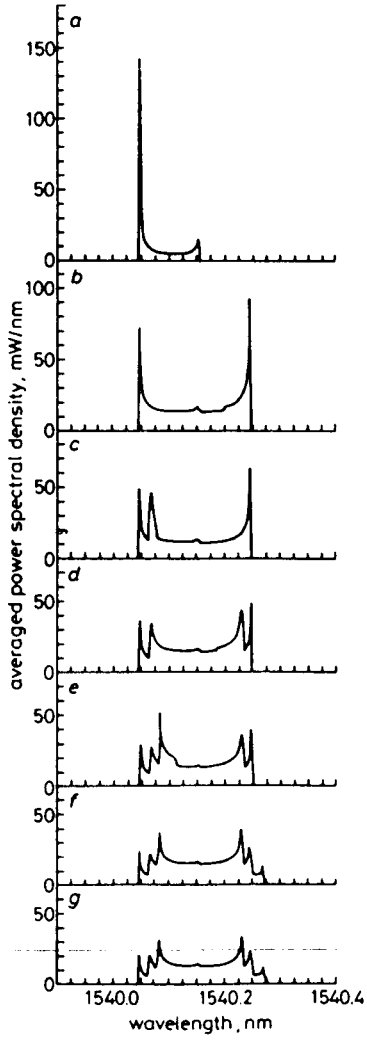

Fig. 5 *Calculated evolution of the total averaged power spectrum of the dominant mode for the same case as Fig. 4*

In each case the starting time for the averaging process was at the beginning of the modulation current pulse, and the final times were as follows: *a* 100 ps, *b* 200 ps, *c* 300 ps, *d* 400 ps, *e* 500 ps, *f* 600 ps, *g* 700 ps.

Fig. 5 brings out a feature which was not easily visible on Fig. 4, namely the shift of maximum wavelength excursion in each successive cycle of the relaxation oscillations. In addition to this shift, we see also an extra long-wavelength spike in Figs. 5*f* and *g* at the end of the modulating pulse. Going through the sequence *a*–*g*, we note the decrease in relative height of the 'rabbit-ear' spikes with respect to the central portion of the spectrum. The characteristic notch seen near the centre of each trace corresponds to the wavelength of the prebias emission. While the results of Fig. 5 bear a resemblance to the experimental measurements of Olsson *et al.* [17], it should be noted that the latter correspond to different modulation currents rather than to different averaging intervals as here. This resemblance comes about since the damped oscillations in our case give rise to an average spectrum (Fig. 5*g*) which emulates the envelope trace (Fig. 1 of Reference 17) generated by the use of different modulation currents.

5 Conclusion

This paper has described the calculation of time-averaged spectra of rapidly-modulated semiconductor lasers. The results are derived from the transient solution of multimode rate equations, including wavelength-chirping effects occurring as a result of the dependence of refractive index on carrier concentration. A numerical averaging procedure has been used to simulate spectra recorded by measuring equipment with a specific time of response. Confining attention to the time-averaged spectrum of the dominant mode, it has been possible to compute curves which show a characteristic 'rabbit-eared' fine structure. The results are in qualitative agreement with experimental measurements reported by other authors [17, 24].

6 Acknowledgments

Dr. Osiński gratefully acknowledges British Telecom Research Laboratories for supporting this work. The Director of Research of British Telecom is thanked for permission to publish.

7 References

1 HAKKI, B.W.: 'Optical and microwave instabilities in injection lasers', *J. Appl. Phys.*, 1980, **51**, pp. 68–73
2 PAOLI, T.L., RIPPER, J.E., and ZACHOS, T.H.: 'Resonant modes of GaAs junction lasers—II. High-injection level', *IEEE J. Quantum Electron.*, 1969, **QE-5**, pp. 271–276
3 BUUS, J., DANIELSEN, M., JEPPESEN, P., MENGEL, F., MOESKJAER, H., and OSTOICH, V.: 'On the dynamic and spectral behaviour of DH GaAlAs stripe lasers modulated with subnanosecond pulses'. Proc. 2nd European Conf. on optical fibre communication, Paris, 1976, pp. 231–239
4 ARNOLD, G., and RUSSER, P.: 'Modulation behaviour of semiconductor injection lasers', *Appl. Phys.*, 1977, **14**, pp. 255–268
5 PAOLI, T.L., and RIPPER, J.E.: 'Coupled longitudinal mode pulsing in semiconductor lasers', *Phys. Rev. Lett.*, 1969, **22**, pp. 1085–1088
6 CHINONE, N., and ITO, R.: 'Spectral behaviors of spontaneously pulsing double-heterostructure injection lasers', *Jpn. J. Appl. Phys.*, 1974, **13**, pp. 575–576
7 ARNOLD, G., and PETERMANN, K.: 'Self-pulsing phenomena in (GaAl)As double-heterostructure injection lasers', *Opt. & Quantum Electron.*, 1978, **10**, pp. 311–322
8 VAN DER ZIEL, J.P.: 'Spectral broadening of pulsating $Al_xGa_{1-x}As$ double heterostructure lasers', *IEEE J. Quantum Electron.*, 1979, **QE-15**, pp. 1277–1281
9 VAN DER ZIEL, J.P., MERZ, J.L., and PAOLI, T.L.: 'Study of intensity pulsations in proton-bombarded stripe-geometry double-heterostructure $Al_xGa_{1-x}As$ lasers', *J. Appl. Phys.*, 1979, **50**, pp. 4620–4637
10 CHIK, K.D., DYMENT, J.C., and RICHARDSON, B.A.: 'Self-sustained pulsations in semiconductor lasers: experimental results and theoretical confirmation', *ibid.*, 1980, **51**, pp. 4029–4037
11 ELISEEV, P.G., MOROZOV, V.N., PASHKO, S.A., SERGEEV, A.B., and SKOPIN, I.A.: 'Broadening of spectral modes of a semiconductor laser in the case of pulsations of the emission intensity', *Sov. J. Quantum Electron.*, 1980, **10**, pp. 1273–1275
12 VAN DER ZIEL, J.P., TSANG, W.T., LOGAN, R.A., MIKULYAK, R.M., and AUGUSTYNIAK, W.M.: 'Subpicosecond pulses from passively mode-locked GaAs buried optical guide semiconductor lasers', *Appl. Phys. Lett.*, 1981, **39**, pp. 525–527
13 YOKOYAMA, H., ITO, H., and INABA, H.: 'Generation of subpicosecond coherent optical pulses by passive mode locking of an AlGaAs diode laser', *ibid.*, 1982, **40**, pp. 105–107
14 VEITH, G., KUHL, J., and GÖBEL, E.O.: 'Temporal and spectral characteristics of rapidly gain-switched GaAs/GaAlAs buried-heterostructure lasers', *Electron. Lett.*, 1983, **19**, pp. 385–387
15 KISHINO, K., AOKI, S., and SUEMATSU, Y.: 'Wavelength variation of 1.6 μm wavelength buried heterostructure GaInAsP/InP lasers due to direct modulation', *IEEE J. Quantum Electron.*, 1982, **QE-18**, pp. 343–351
16 OSIŃSKI, M., and ADAMS, M.J.: 'Intrinsic manifestation of regular pulsations in time-averaged spectra of semiconductor lasers', *Electron. Lett.*, 1984, **20**, pp. 525–526
17 OLSSON, N.A., DUTTA, N.K., and LIOU, K.-Y.: 'Dynamic linewidth of amplitude-modulated single-longitudinal-mode semiconductor lasers operating at 1.5 μm wavelength', *ibid.*, 1984, **20**, pp. 121–122
18 ASPIN, G.J., and CARROLL, J.E.: 'Gain-switched pulse generation with semiconductor lasers', *IEE Proc. I, Solid State and Electron Dev.*, 1982, **129**, pp. 283–290
19 CAMERON, K.H., CHIDGEY, P.J., and PRESTON, K.R.: '102 km optical fibre transmission experiments at 1.52 μm using an external cavity controlled laser transmitter module', *Electron. Lett.*, 1982, **18**, pp. 650–651
20 LIU, P.-L., LIN, C., KAMINOW, I.P., and HSIEH, J.J.: 'Picosecond pulse generation from InGaAsP lasers at 1.25 and 1.3 μm by electrical pulse pumping', *IEEE J. Quantum Electron.*, 1981, **QE-17**, pp. 671–674
21 LIN, C., TOMITA, A., TYNES, A.R., GLODIS, P.F., and PHILEN, D.L.: 'Picosecond dispersionless transmission of InGaAsP injection laser pulses at the minimum chromatic dispersion wavelength in a 27 km-long single-mode fibre', *Electron. Lett.*, 1982, **18**, pp. 882–884
22 LIN, C., LEE, T.P., and BURRUS, C.A.: 'Picosecond frequency chirping and dynamic line broadening in InGaAsP injection lasers under fast excitation', *Appl. Phys. Lett.*, 1983, **42**, pp. 141–143
23 KOYAMA, F., ARAI, A., SUEMATSU, Y., and KISHINO, K.: 'Dynamic spectral width of rapidly modulated 1.58 μm GaInAsP/InP buried-heterostructure distributed-Bragg-reflector integrated-twin-guide lasers', *Electron. Lett.*, 1981, **17**, pp. 938–940
24 LINKE, R.A.: 'Transient chirping in single-frequency lasers: Lightwave systems consequences', *ibid.*, 1984, **20**, pp. 472–474
25 OSIŃSKI, M., and ADAMS, M.J.: 'Computer simulated transient evolution of 1.55 μm laser spectra'. Proc. 8th ECOC (European Conference on optical communication), Cannes, 1982, pp. 169–173
26 ADAMS, M.J., and OSIŃSKI, M.: 'Longitudinal mode competition in semiconductor lasers: Rate equations revisited', *IEE Proc I, Solid State and Electron Dev.*, 1982, **129**, pp. 271–274
27 OSIŃSKI, M., and ADAMS, M.J.: 'Gain spectra of quaternary semiconductors', *ibid.*, 1982, **129**, pp. 229–236
28 TURLEY, S.E.H.: 'Anomalous effect of carriers on dielectric constant of (In, Ga) (As, P) lasers operating at 1.3 μm wavelength', *Electron. Lett.*, 1982, **18**, pp. 590–592
29 MANNING, J., OLSHANSKY, R., and SU, C.B.: 'The carrier-induced index change in AlGaAs and 1.3 μm InGaAsP diode lasers', *IEEE J. Quantum Electron.*, 1983, **QE-19**, pp. 1525–1530
30 BOULEY, J.-C., CHARIL, J., SOREL, Y., and CHAMINANT, G.: 'Injected carrier effects on modal properties of 1.55 μm GaInAsP lasers', *ibid.*, 1983, **QE-19**, pp. 969–974
31 HSIEH, J.J., and SHEN, C.C.: 'Room-temperature CW operation of buried-stripe double-heterostructure GaInAsP/InP diode lasers', *Appl. Phys. Lett.*, 1977, **30**, pp. 429–431
32 WYATT, R., SMITH, D.W., and CAMERON, K.H.: 'Megahertz linewidth from a 1.5 μm semiconductor laser with HeNe laser injection', *Electron. Lett.*, 1982, **18**, pp. 292–293
33 VAN DER ZIEL, J.P., TEMKIN, H., and LOGAN, R.A.: 'Quaternary 1.5 μm (InGaAsP/InP) buried crescent lasers with separate optical confinement', *ibid.*, 1983, **19**, pp. 113–115
34 HENNING, I.D.: 'Linewidth broadening in semiconductor lasers due to mode competition noise', *ibid.*, 1983, **19**, pp. 935–936